Defence Life Science Journal, Vol. 10, No. 2, April 2025, pp. 111-120, DOI : 10.14429/dlsj.20245

Characterisation, Synthesis, and Antimicrobial Activities of Silver Nanoparticles Formed via Green Synthesis Approach using Aqueous Extract derived from the Bark of *Mangifera indica*: A Sustainable Resource

Shalini Tailor[#], Ayushi Malik[#], R.K. Gaur[$] and Avinash Marwal[#,*]

[#]*Nanoparticle Synthesis and Bioinformatics Laboratory, Department of Biotechnology, Vigyan Bhawan, Block-B, New Campus, Mohanlal Sukhadia University, Udaipur, Rajasthan - 313 001, India*

[$]*Department of Biotechnology, Deen Dayal Upadhyay Gorakhpur University, Gorakhpur, Uttar Pradesh - 273 009, India*

[*]*E-mail: marwal_avinash@yahoo.co.in*

ABSTRACT

Many research opportunities have arisen as a result of the green synthesis method for nanoparticle creation and the rapid development and breakthroughs in nanotechnology. This study covers the one-step synthesis of silver nanoparticles (SNPs) from *Mangifera indica* bark aqueous extracts. Bark extract is combined with $AgNO_3$ to perform green synthesis of SNP. The synthesised SNPs were characterised by a color change from light yellow to deep brown, as well as UV-VIS spectrophotometry in the 300-700 nm area. Further characterisations were carried out using Fourier transform infrared spectroscopy (FTIR) and X-Ray Diffraction (XRD) studies, followed by Scanning Electron Microscopy (SEM) and Energy-Dispersive X-ray spectroscopy (EDX) analysis. Phytochemical examination of crude bark extract revealed the existence of secondary metabolites alkaloids, flavonoids, phenolics, tannins, and saponins but no glycosides and starch were present. The antimicrobial activity (AMA) of Bark SNP (BSNP) towards gram-positive bacteria [*Staphylococcus Aureus* (SA) & *Streptococcus Pyogenes* (SP)], gram-negative bacteria [*E. coli* (EC) & *Pseudomonas aeruginosa* (PA)], and *Candida* species were determined using the disc diffusion technique. A single-factor ANOVA was used for performing the statistical analysis, and p-values < 0.05 designated statistical significance. The green synthesised SNPs were spherical and crystal size ranged between 10 and 12 nm on average. In UV-vis spectroscopy, the absorption spectra peaked at 460 nm. It was discovered that the SNPs' antibacterial activity was stronger than their antifungal activities. Compared to commercial medicines, the BSNP exhibits a reasonable inhibitory effect. The purpose of the current study was to build a new, affordable, ecologically safe process for a plant-mediated green approach for SNP synthesis and evaluate its antimicrobial activity for sustainable resources.

Keywords: Nanotechnology; Green synthesis; Silver nanoparticles; *Mangifera indica* bark; Antimicrobial activity

NOMENCLATURE

AMA : Antimicrobial activity
BSNP : Bark silver nanoparticles
DIW : De-ionized water
EC : *Escherichia coli*
EDX : Energy-Dispersive X-ray spectroscopy
FCC : Face centre cubic
ICDD : International centre for diffraction data
MHA : Mueller-Hinton agar
MTCC : Microbial type culture collection
NPs : Nanoparticles
PA : *Pseudomonas aeruginosa*
SA : *Staphylococcus aureus*
SP : *Streptococcus pyogenes*
SDA : Sabouraud dextrose agar
SNPs : Silver nanoparticles
ZOI : Zone of inhibition

1. INTRODUCTION

In 1974, N. Taniguchi coined the word "nanotechnology," which refers to the study of the creation and application of particles ranging in size from 1 to 100 nm, or 1×10^{-9} m[1]. Chemical, physical, or biological procedures are the three ways that nanotechnology is used to synthesise nanoparticles (NPs)[2,3]. Numerous sectors, including forestry, agriculture, drug delivery, pharmaceuticals, plant disease control, etc., employ the use of nanotechnology [4]. Due to their high surface-to-volume ratio, which denotes for their enhanced reactivity and biochemical activities, NPs are currently favoured over other chemical formulations[5]. Raveendram[6], *et al.* pioneered green mode nanoparticle synthesis, wherein silver nanoparticles were synthesised by reducing β-D-glucose and using starch as the capping agent. The goal of green nanoparticle synthesis was to reduce the harmful consequences of chemically manufactured nanoparticles while also producing biologically useful and cost-effective ones. Green-mediated nanoparticle production and characterisation have developed as a key area of nanotechnology, particularly for noble metals like Pd (Palladium), Ag (Silver), Au (Gold), and Pt (Platinum)[7]. Most widely used metal nanoparticles

Received : 30 May 2024, Revised : 21 December 2024
Accepted : 13 January 2025, Online published : 07 April 2025

developed and utilised are obtained from Silver and named as Silver Nanoparticles (SNPs). Silver (Ag) has high antibacterial properties and a specific surface area for maximum environmental contact[8]. Silver is the most widely utilised noble metal due to its wound-healing properties and application in biomedicine.

Plant components include a variety of phytoconstituents that work to reduce metallic compounds into metallic particles at the nanoscale[9]. High levels of antioxidant activity are found in active bioactive chemicals found in *Mangifera indica*[10]. *M. indica* tree phytochemicals possess antibacterial and antiviral qualities because they possess substances like phenolic compounds[11]. Ethanolic extract derived from *M. indica* fruit kernel has a high antibacterial activity as shown against a variety of pathogenic bacteria, such as *Streptococcus pyogenes, Pseudomonas aeruginosa, Klebsiella pneumoniae, and Staphylococcus aureu* [12]. *M. indica*, an ancient tree with huge medicinal properties, has been utilised in several ways. Research on *M. indica* fruit has demonstrated their anti-enteric[13], antibacterial[14], antidiarrheal[15], and antioxidant effects[16].

Every part of the *M. indica* tree possesses some or the other kind of medicinal properties. Most research work has been done on leaves[17-18], mango pulp[19-20], seeds[21], and peels[22-23] but the bark has not been explored for its beneficial properties. Hence, the current study examines the advantages of nanotechnology with the bark of *Mangifera indica* for the biosynthesis of SNPs and to detect its antimicrobial activity against a group of microbes. The phytoconstituents of bark work as the reducing as well as the capping agent for the generation of SNPs[24]. Because of the fast growth of nanostructured noble metals and their utilisation in medicine, the goal of this work focuses on the biogenic creation of SNPs utilising the aqueous extract derived from the bark of *M. indica*, which has a variety of therapeutic benefits and may prove to be a sustainable resource in the near future. The phytochemical composition of the *M. indica* bark extract is qualitatively analysed and the created SNPs was quantitatively characterised by UV-VIS, FTIR, SEM, XRD, etc.

2. MATERIAL AND METHODS

2.1 Chemicals and Materials

All the chemicals used were purchased from HiMedia Pvt. Ltd. (Mumbai, India) and deionised water (DIW) was used throughout the experiment. The collection of bark (~5-6 inches pieces) was done from the mango orchards (2-3 years old) of Krishi Vigyan Kendra, Banswara, Rajasthan, India (23.54 ºN, 74.433 ºE). The species was identified in the University of Rajasthan's Botany Department Herbarium in Jaipur, Rajasthan, India (RUBL 21398). The following microbial strains were purchased from the Microbial Type Culture Collection and Gene Bank (MTCC) in Chandigarh: *S. pyogenes* (MTCC 442), *C. glabrata* (MTCC 3019), *S. aureus* (MTCC 96), *E. coli* (MTCC 729), *C. albicans* (MTCC 3017) and *P. aeruginosa* (MTCC 3541).

2.2 Preparation of Plant Extract

The bark was isolated from a fully mature and fruiting mango tree from the upper, middle, and lower regions of the trunk in February-March. The circumference of the trunk was 3-4 meters. The bark was light to dark brown in colour and had a rough appearance. The bark samples were mixed together before carefully cleaned multiple times with DIW to remove dirt and shade dried for 1 week. The bark was pulverised into fine powder by crushing, and grinding using pestle mortar and grinder followed by sieving with the muslin cloth. 2 grams of bark powder were combined with 100 millilitres of DIW. The mixture was placed in a 60 °C water bath for 30 minutes before being agitated for one hour on a magnetic stirrer. The combination was then filtered by means of Whatman Filter Paper no.1 and was reserved at 4 °C until the next usage.

2.3 Biogenic Formation of Silver Nanoparticles

In deionized water, 20 ml of bark extract and 80 ml of 1 mM $AgNO_3$ were combined (Niraimathi[35], *et al.* 2013). To reduce the photo-activation of $AgNO_3$, the entire reaction was conducted in low light. The solution changed color briefly, going from light to reddish-brown to deep brown, suggesting that $AgNO_3$ has been reduced to SNPs. Additionally, a UV-visible spectrophotometer was employed to characterise the solution's spectrum. The reaction mixture was centrifuged for 15 minutes at 4 °C and 5000 rpm. The pellets were collected and dehydrated at 40 °C in the oven to obtain BSNPs.

2.4 Qualitative Analysis of Bark Extract for Phytochemicals

The aqueous extract of bark was tested for phytoconstituents including flavonoids, alkaloids, reducing sugars, glycosides, saponins, phenols, tannins, starch, steroids, and proteins, using a standard procedure mentioned by Shaikh and Patil[25].

2.5 Statistical Analysis

The biological studies were performed in a set of triplicates and independently three times. The results were represented as mean ± SD. The data was assessed with a single-factor analysis of variance (ANOVA), with statistical significance determined as $p < 0.05$.

2.6 Antimicrobial Assay of Bark SNP

To develop freshly acquired microbial strains, they were placed in Nutrient Broth (NB). The cultures were then incubated for 18 to 24 hours at 37 °C. In addition, the cultures were cultivated on Nutrient Agar (NA). After an overnight growth period in the NB, the cultures

were tested for viability and microbial culture density using the O.D. (Optical Density) between 0.5-1. In parallel, previously established processes were employed to manufacture sterilised MHA and SDA plates for AMA[26-28]. After the media solidified, the overnight cultures of the two fungal strains (CA & CG) and four bacterial strains (SA, SP, EC & PA) were spread out on agar petri dishes with the help of a disinfected cotton swab. Here, the 5 mm sterile paper discs were used in the disc diffusion test and labelled with the appropriate concentration. Paper discs inoculated with 1 mM $AgNO_3$, 50 µl of BSNP1, 100 µl of BSNP2, and the crude extract of Bark were used in the current study. The paper discs were evenly spaced and placed throughout the infected plates after being allowed to air dry for a portion of their length. In these antimicrobial plates, fluconazole and ampicillin were used as positive controls, while paper discs soaked in autoclaved water were used as negative controls. After 24 to 36 hours, the antimicrobial actions were determined by calculating the diameter of the clear Zone of Inhibition (ZOI) encircling the discs. The experiments were done thrice independently. To measure the antimicrobial action, the mean ZOI diameters (mm) of the SNP were investigated.

3. CHARACTERISATION

By diluting the sample with deionized water as a reference, UV-vis analysis (Shimadzu-1900i series) was carried out by scanning between 300 and 700 nm range. To ensure that the results were precise, reliable, and free of contamination, all necessary steps have been taken to maintain sterility. Centrifugation was done for 15 minutes at 5000 rpm to purify the BSNP solution. Purified SNPs were dried, and then their composition and structure were examined using FTIR, SEM, XRD, and EDX before being further investigated for an antibacterial assay. XRD was used to determine the BSNP's nature and particle size. The Bruker AXS D8 Advance X-ray diffractometer, having a current and voltage array of 30 mA and 40 kV, was employed for this. Cu kα was employed, and its wavelength was 0.154 nm. Following the fine powdering of the material used in the experiment, the usual bulk configuration was investigated. The scanning time ranged between 20 and 90 seconds. To interpret the crystalline structure, the observed peaks were verified using the ICDD (International Centre for Diffraction Data) library. Debye Scherrer equations were employed to calculate the element or grain size of the BSNPs.

Crystalline size, D= K / cos

where D is the observed peak angle degree, K represents crystalline-shape factor (0.9), B denotes for X-ray diffraction broadening (Full Width at half maximum) radian; λ stands for X-ray wavelength (1.540598) nm. FTIR spectroscopy was accomplished via the Bruker FTIR Alpha spectrophotometer. In the transmission mode, the FTIR spectrums were detected between 4000 and 400 cm^{-1} keeping the spatial resolution at 4 cm^{-1}. The samples were generated using the KBr pellet process, and the surface chemistry of the reduced silver ion was determined, as well as the existence of any bio-functional groups in the samples under study. The Carl Zeiss Gemini SEM300 FE-SEM was utilised for Energy Dispersive X-ray (EDX) analysis along with SCANNING ELECTRON MICROSCOPY. Fine particles of the tested sample were deposited straight onto the aluminum stub with carbon tape on top and then stowed within the equipment for inspection. The antibacterial capabilities of the biosynthesised silver nanoparticles were assessed towards gram-positive (SA and SP), gram-negative (EC and PA), and fungal strains of *Candida spp*. by the standard disc-diffusion method. Ampicillin and fluconazole were employed as the standard drug (positive control) for AMA, and the Zone of Inhibition (ZOI) during the sensitivity test was assessed. The autoclaved MHA and SDA media were used to cultivate the bacterial and fungal cultures, respectively.

4. RESULTS AND DISCUSSION

4.1 Biogenic Formation of Bark Silver Nanoparticles

The bark of *M. indica* showed a colour shift from light reddish brown to dark brown on mixing the aqueous bark extract with a 1 mM $AgNO_3$ blend (Fig. 1), indicating the creation of nanoparticles. The visual aspect of the reaction blend changed from light brown to dark reddish-brown as a result of BSNP surface plasmon resonance, i.e. regarded to be the chief indicator of nanoparticle creation. Comparable outcomes were determined by Bharathi[29], *et al.* and Kora[30], *et al.* during the biogenic formation of SNPs from *M. indica* and *O. sativa* leaf extract.

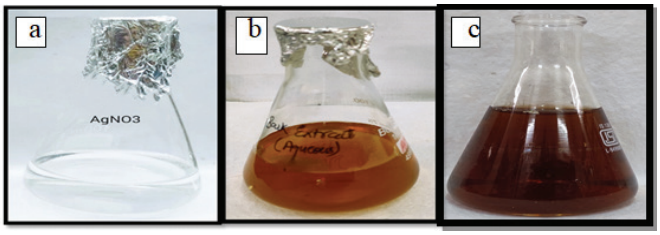

Figure 1. Color change observed after adding (a) AgNO3 to (b) bark extract forming (c) BSNP.

4.2 Qualitative Phytochemical Screening

Phytochemicals are the most efficient biological resources for producing metallic nanoparticles. Solvable phytochemicals such as flavonoids, quinones, organic acids, and polyphenols mostly contribute towards quick reduction of silver ions[31]. Bark aqueous extract was subjected to phytochemical screening, which identified alkaloids, flavonoids, phenolics, and saponins as the compounds that seem to be responsible for the creation of nanoparticles (Table 1).

4.3 UV-VIS Spectroscopy

When *M. indica* bark extract was utilised as a reducing agent and the samples were glanced from 300 to 700 nm employing a UV-visible spectrophotometer, a

rapid bio-reduction of silver nitrate was observed. 460 nm was the wavelength of the UV–visible spectrum exhibiting the characteristic peak for silver nanoparticles (Fig. 2). For further characterisation, these biosynthesised nanoparticles were used.

Table 1: Phytochemical analysis of the crude aqueous extract of bark

S. No.	Phytochemicals test		End result	Presence / absence
1	Alkaloids	Mayer's reagent	Reddish-brown ppt. or colouration	+
2	Flavonoids	Alkaline reagent	Yellow colour changes to colourless	+
3	Glycosides	Keller-Killani test	Green-blue colour	-
4	Phenolics	Ferric chloride test	Colour change observation after adding base	+
5	Proteins	Xanthoproteic test	Yellow to Deep orange colour	+
6	Saponins	Foam Test	Froth formation at the surface	+
7	Starch	Starch Test	Bluish-black ppt	-
8	Steroids	Hesse's Test	Reddish-brown colour	+
9	Sugars	Fehling's test	Greenish colour changing to red	+
10	Tannins	Braymer's test	Blue or greenish colour	+

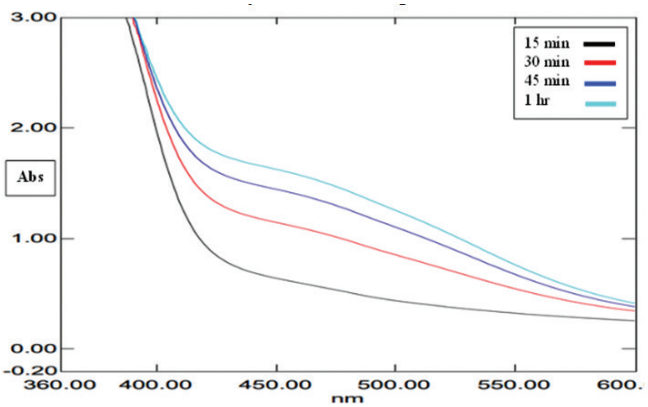

Figure 2. UV-VIS spectra of bark SNP.

4.4 X-Ray Diffraction Analysis (XRD)

X-ray diffraction outline of BSNP, as revealed in Fig. 3, indicates that the subjected material is crystalline and in one phase. The ICDD card no. 03-0921, 04-0784, and 87-0720 were used to determine the existence of just Ag. Additionally, the size of the nanoparticle crystallites was exhibited using Scheler's Formula (Table 2). It was discovered that the produced nanoparticle values ranged from 9 to 11 nm. The silver phase indicated that it contains a significant number of nano Ag-particles, and is responsible for the greatest intense peak, which is located at 38.21º. Generally, particle size effects are responsible for the widening of peaks in solids' XRD patterns. Larger peaks indicate lower particle sizes and show how the development and nucleation of the crystal nuclei are impacted by the experimental circumstances[32]. The silver facets (111), (200), (311), and (222) (Fig. 3) have peaks at four different planes that correspond to their 2θ are 38.21º, 44.22º, 64.68º, and 77.44º in accordance to Face Center Cubic (FCC) crystal assembly of BSNPs. Tripathy[33], *et al.* and also Donga and Chanda[34] reported a similar discovery in their investigations.

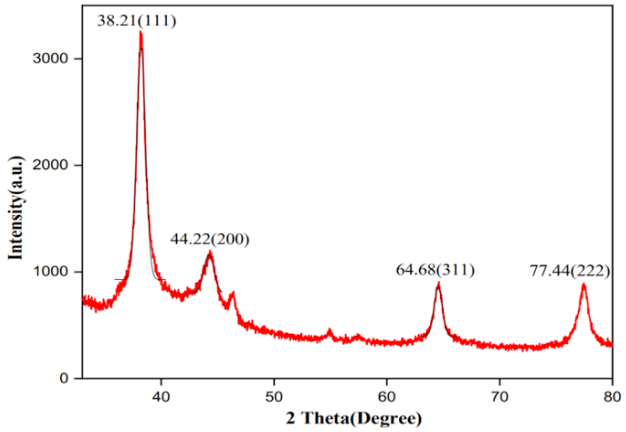

Figure 3. X-ray diffraction analysis of generated bark SNP.

Table 2. XRD examination of bark derived SNP by scherer's formula.

S. No.	Peak value (2Theta)	Fwhm	Hkl value (Mi)	Crystal vize Nm (D)	Average size (D)
1	38.21	0.94451	111	9.31	10.08nm
2	44.22	0.90812	200	9.91	
3	64.68	0.97887	311	10.04	
4	77.44	0.96018	222	11.08	

4.5 Fourier Transform Infrared Spectroscopy Analysis (FTIR)

The existence of O-H bond area and H-bonded phenols & alcohols were indicated by the peak in the FTIR spectrum, which was observed at 3429/cm. There is evidence of the O-H stretch of carboxylic acids at 2928/cm. According to Fig. 4, the N-H curve of primary

amino acids and the C-H curve of alkanes happened at 1639/cm and 1350/cm, correspondingly. According to earlier research, this N-H bend is in charge of SNP stability[35]. The aromatic and primary alcohols are represented by the C-O extending at 1078/cm. Alkene's C-H turn appeared to be a faint stretch at 825/cm. The crests at 3469/cm and 2928/cm were ascribed to O-H bounded area of polyphenolic compounds and C-H stretching of proteins, correspondingly[36-37]. Alkaloids, tannins, phenolics, saponins, steroids, flavonoids, and sugars were all present in the *M. indica* bark powder[34]. These essential secondary metabolites may have a major impact on the synthesis, reduction, capping, and stabilisation of SNPs. A similar study demonstrated that proteins and phenolic substances help fruit extract reduce silver ions to silver nanoparticles, aligning with our finding[38]. As functional groups, they included phenol or alcohol, alky[l] halides, alkynes, carboxylic acid, ketones, amines, aromatics, and aliphatic amines. This is in line with our findings.

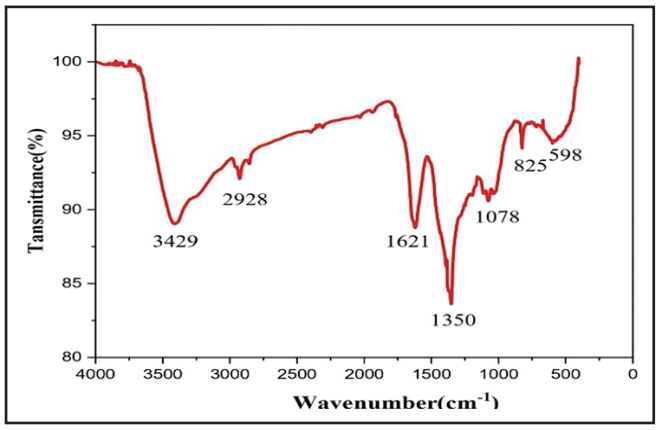

Figure 4. FTIR spectrum of bark SNP.

4.6 Scanning Electron Microscopy (SEM) and Energy Dispersive X-ray (EDX) Analysis

Analysing resulting image of the biosynthesised silver sample, certain unevenly granulated fused agglomerates of powder with brighter facets can be observed, along with polymorphic morphologies such as spherical, ellipsoidal, and cubical. The SNPs' aggregation as a result of centrifugation is the cause of their phenomenal size (Fig. 5a). Energy dispersive X-ray analysis, which is housed inside the SEM apparatus, was utilised to determine the elemental composition of the biosynthesised SNPs, which mostly include elemental silver in considerable quantities with tiny levels of carbon and oxygen as contaminants.

Additionally, not a single extra element was found via the scan rate approach as observed in the EDX (Fig. 5b)[39], surface plasmon resonance in metallic silver nanocrystals produces a noticeable signal at 3 keV. The phytoconstituents such as cardiac glycosides, flavonoids, alkaloids, tannins, etc. that are present in the nanoparticles during their biosynthesis also vary in size and form depending on the plant and portion employed[40].

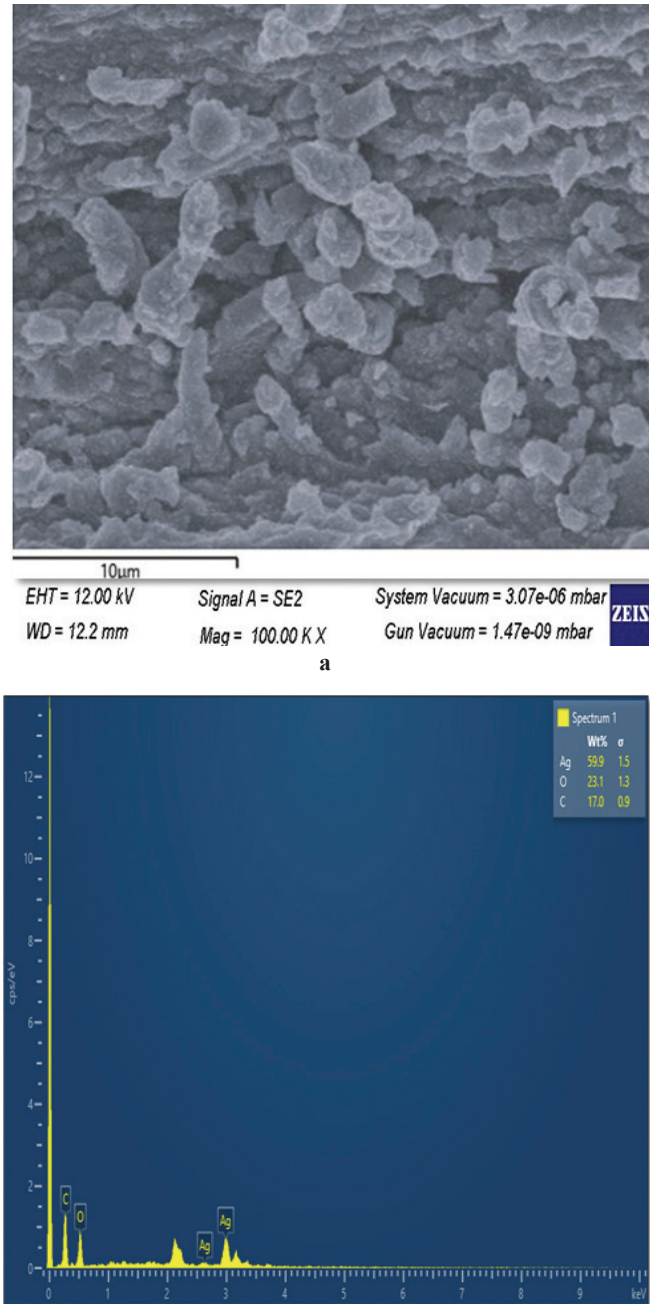

Figure 5. Scanning Electron Microscopy micrograph (a) and Energy Dispersive X-ray spectrum (b) of elemental composition of Bark SNP.

4.7 Disc Diffusion Approach for Antimicrobial Studies

Disc diffusion protocols were employed to assess the bark SNP's antibacterial activity, adhering to the preceding section's protocol. On the plates, SNPs showed greater antibacterial action towards Gram-negative (PA and EC) bacteria in contrast to Gram-positive (SA and SP) bacteria. Comparable to ampicillin (10µg disc) in terms of effectiveness, BSNP1 (100 µl) outperformed BSNP2 (50 µl). Zone of inhibition was detected in the antibacterial activity of gram-positive (SA and SP) and gram-negative (EC and PA) bacteria, the antifungal activity of the biosynthesised SNP from bark extract

against *Candida Albicans* (CA), and *Candida glabrata* (CB) was also observed. SNPs showed low antifungal action but greater antibacterial action towards both Gram-positive and Gram-negative bacteria, as shown in Fig. 6(a) and (b) represented as the ZOI by the antibiotic, BSNP1 and BSNP2, $AgNO_3$, and crude bark extract (Fig. 7 and Fig. 8).

Comparable to fluconazole (10µg disc) in terms of effectiveness, more antifungal activity was shown by *C. albicans* than by *C. glabrata*. The ZOI (mm) measurement was determined using Vernier callipers and related controls as shown in Table 3. The absence of a zone of inhibition in the control DW attested to the procedure's correct execution. Gram-negative bacteria showed additional response to nanoparticle-induced antimicrobial actions in contrast to Gram-positive bacteria. Gram positive and Gram-negative bacteria easily distinguishable from one another by their unique cell wall compositions. According to Kokila[41], *et al.* gram-positive bacteria possess thicker peptidoglycan coating on its cell walls than do gram-negative bacteria own. The type of bacteria and the concentration of nanoparticles affect the antimicrobial efficiency[42].

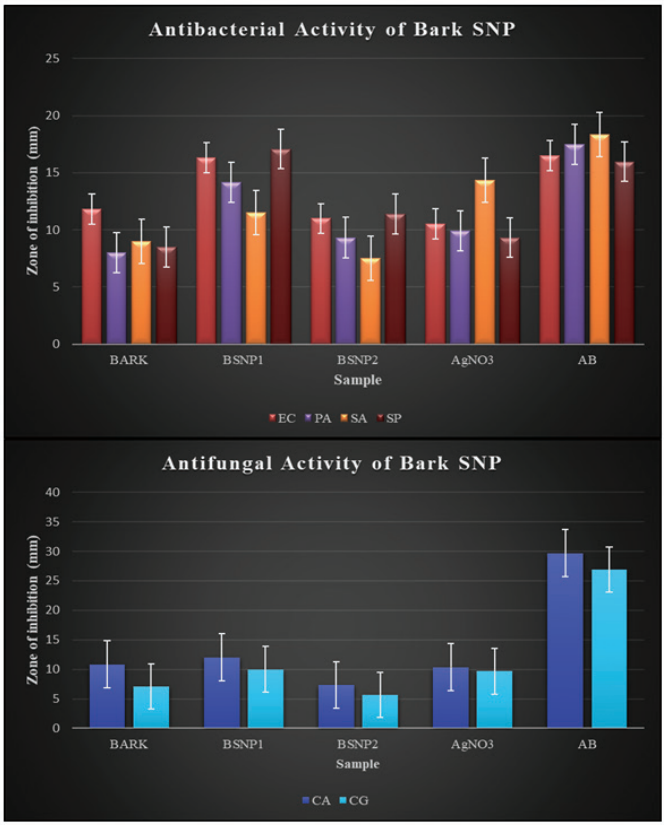

Figure 6. Antimicrobial action of bark SNP towards bacteria (a) and fungus (b).

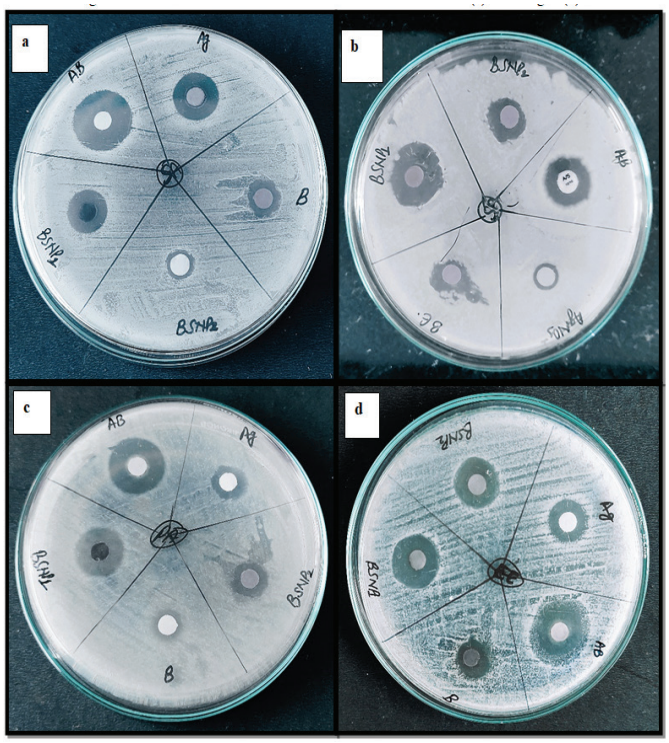

Figure 7. Antibacterial Activity of Bark SNP against Gram-Positive (a=SA & b=SP) & Gram-Negative (c=PA & d=EC) bacteria (BSNP1=100µl, BSNP2=50µl, AgNO3=1mM, B=Bark extract crude, AB=Ampicillin (10µg disc)]

Table 3. Antimicrobial activity represented by zone of inhibition (mm), (Represented as Mean + SD)

Microbes	Bark Extract	BSNP1 (100µl)	BSNP2 (50µl)	$AgNO_3$ (1 mM)	AB (10µg)
EC	11.83 ± 0.28	16.33 ± 0.57	11 ± 1	10.55 ± 0.5	16.5 ± 0.5
PA	8 ± 1	14.16 ± 0.76	9.33 ± 0.28	9.9 ± 0.173	17.5 ± 0.5
SA	9 ± 1	11.51 ± 0.5	7.5 ± 0.5	14.33 ± 0.57	18.33 ± 1
SP	8.5 ± 0.5	17.08 ± 0.62	11.4 ± 0.36	9.33 ± 0.57	15.96 ± 0.25
CA	10.83 ± 0.28	12 ± 0.5	7.33 ± 0.28	10.33 ± 0.57	29.67 ± 0.57
CG	7.06 ± 0.3	10 ± 0.3	5.67 ± 0.57	9.67 ± 0.57	26.9 ± 0.45

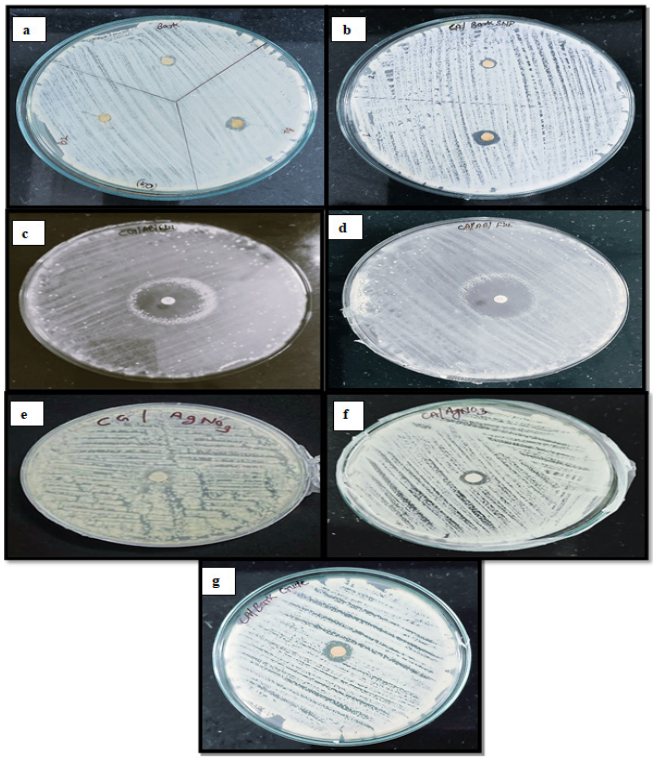

Figure 8. Antifungal Activity of Bark SNP against Candida glabrata (CG=A, C, E) & Candida albicans (CA=B, D, F, G) [BSNP1=100µl, BSNP2=50µl, AgNO3=1mM, B=Bark extract crude, AB=Fluconazole (10µg/disc)].

5. CONCLUSION AND FUTURE DIRECTIONS

Because of their unique structure and small size, nanomaterials have attracted a lot of interest from researchers lately. Significant advancements have been made in the areas of biomolecule delivery in animal cells, diagnostics, and therapies[43]. Nonetheless, nanotechnology's use in plant research is still in its infancy. A significant increase in agricultural output might result from the significant prospects that nanotechnology offers to improve crop yield[44]. Broad advances in agricultural research are made possible by nanotechnology, including in fields like reproductive science and technology, enzymatic nano-bioprocessing, which turns food and agricultural waste into energy and other useful byproducts, and the use of different nanocides to prevent and treat plant diseases[45]. *M. indica* derived bark extract was employed in the current investigation to produce BSNPs, and it efficiently converted $AgNO_3$ to NPs. This preparation method of nanoparticle is safe, low-cost, and naturally friendly. There is good concordance between the standard ICDD cards and the powder XRD data acquired on silver nanoparticles synthesized. The sample showed crystalline Face-Centered Cubic (fcc) lattice structures of elemental silver, according to the XRD pattern. The silver nitrate solution was actively reduced to BSNPs by *M. indica*, as demonstrated by the positive bio-reduction zones in the FT-IR measurements. Due to a high Surface Plasmon Resonance (SPR) value observed between wavelengths of 400 and 460 nm, UV–vis spectroscopy verified the existence of SNPs. The SEM image revealed the presence of compact, high-density agglomerates of silver particles, as well as the formation of various highly agglomerated structures with polymorphic shapes such as spherical, ellipsoidal, and cubic. The elemental analysis of SNPs confirmed the presence of elemental silver with trace amounts of carbon and oxygen as impurities, and the EDXA scan revealed no other elements, indicating the purity of the synthesised sample. After being tested against *S. aureus, S. pyogenes, E. coli, P. aeruginosa, C. albicans*, and *C. glabrata*, it was discovered that the produced nanoparticles were far more potent against the bacteria than the fungus. Additionally, it may be assumed that higher dosages of SNPs will result in greater antibacterial efficacy. Therefore, it can be concluded from the aforementioned study that BSNPs made from *M. indica* bark extract can function as a strong antimicrobial agent against infections that affect humans. It may be inferred from the instance of bacterial activity that SNP can be effectively utilised, and that these metallic nanoparticles, when combined with plant metabolites that have a high antioxidant content, can be employed as a successful substitute for synthetic pharmaceuticals and help address the drug problem. The biosynthesis of SNPs from the bark of the mango plant is a one-step synthesis approach reported from India in this study and can serve as a better and sustainable resource for humankind to curb several diseases. This area of research needs to be explored further.

REFERENCES

1. Yakkala, G.L; & Rao, M. Antibacterial activity of plant extracts and silver mediated nanoparticles of *Ipomoea pescaprae* and *Spinifex littoreus*. *Int. J. Bio-pharma Res*., 2019, **8**(3), 2514–2517. doi: 10.21746/ijbpr.2019.8.3.4
2. Das, A.K.; Marwal, A.; Sain, D. & Pareek, V. One-step green synthesis and characterisation of plant protein-coated mercuric oxide (HgO) nanoparticles: Antimicrobial studies. *Int. Nano Lett*., 2015, **5**(3), 125–132. doi: 10.1007/s40089-015-0144-9
3. Kumar, P.; Senthamil Selvi, S.; Lakshmi Prabha, A.; Prem Kumar, K.; Ganeshkumar, R.S. & Govindaraju, M. Synthesis of silver nanoparticles from *Sargassum tenerrimum* and screening phytochemicals for its antibacterial activity. *Nano Biomed. Eng*., 2012, **4**(1), 12-16. doi: 10.5101/nbe. v4i1.p12-16
4. Das, A.K.; Marwal, A.; Pareek, V.; Joshi, Y. & Apoorva, A. Surface engineering of magnetite nanoparticles by plant protein: Investigation into magnetic properties. *Nano Hybrids Compos*., 2016, **11**, 38-44. doi: 10.4028/www.scientific.net/nhc.11.38
5. Patil, A.; Mishra, V.; Thakur, S.; Riyaz, B.; Kaur, A.; Khursheed, R.; Patil, K. & Sathe, B. Nanotechnology derived nanotools in biomedical perspectives: An update. *Curr. Nanosci*., 2019, **15**(2), 137–146.

6. Raveendran, P.; Fu, J. & Wallen, S.L. Completely "green" synthesis and stabilisation of metal nanoparticles. *J. Am. Chem. Soc*., 2003, **125**(46), 13940-13941.
7. Aritonang, H.F.; Koleangan, H. & Wuntu, A.D. Synthesis of silver nanoparticles using aqueous extract of medicinal plants' (*Impatiens balsamina* and *Lantana camara*) fresh leaves and analysis of antimicrobial activity. *Int. J. Microbiol*., 2019, 8642303. doi: 10.1155/2019/8642303
8. Jyoti, K.; Baunthiyal, M. & Singh, A. Characterisation of silver nanoparticles synthesised using *Urtica dioica* Linn. Leaves and their synergistic effects with antibiotics. *J. Radiat Res. Appl. Sc*., 2016, **9**(3), 217-227. doi: 10.1016/j.jrras.2015.10.002
9. Anandalakshmi, K.; Venugobal, J. & Ramasamy, V.J.A.N. Characterisation of silver nanoparticles by green synthesis method using *Pedalium murex* leaf extract and their antibacterial activity. *Appl. Nanosci*., 2016, **6**, 399-408. doi: 10.1007/s13204-015-0449-z
10. Torres-León, C.; Rojas, R.; Contreras-Esquivel, J.C.; Serna-Cock, L.; Belmares-Cerda, R.E. & Aguilar, C.N. Mango seed: Functional and nutritional properties. *Trends Food Sci. Technol*., 2016, **55**, 109-117. doi: 10.1016/j.tifs.2016.06.009
11. Ribeiro, S.M.R.; & Schieber, A. Bioactive compounds in mango (*Mangifera indica* L.). In Bioactive foods in promoting health. *Academic Press*., 2010, 507-523. doi: 10.1016/B978-0-12-374628-3.00034-7
12. Ahmed, E.F. Antimicrobial and antibiofilm activity of mango seeds extract. *Iraqi. J. Sci*., 2015, **56**(4B), 3121-3129.
13. Rajan, S.; Thirunalasundari, T. & Jeeva, S. Anti-enteric bacterial activity and phytochemical analysis of the seed kernel extract of *Mangifera indica* Linnaeus against *Shigella dysenteriae* (Shiga, corrig.) Castellani and Chalmers. *Asian Pac. J. Trop. Med*., 2011, **4**(4), 294-300. doi: 10.1016/S1995-7645(11)60089-8
14. Engels, C.; Gänzle, M.G. & Schieber, A. Fast LC-MS analysis of gallotannins from mango (*Mangifera indica* L.) kernels and effects of methanolysis on their antibacterial activity and iron binding capacity. *Food Res. Int*., 2012, **45**(1), 422-426. doi: 10.1016/j.foodres.2011.11.008
15. Azhagesan, G.; Rajan, S. & Soranam, R. Anti-Salmonella activities of *Mangifera indica* seed kernel aqueous extract (MISKAE). *Adv. Appl. Sci. Res*., 2015, **6**, 75-80.
16. Lim, K.J.A.; Cabajar, A.A.; Lobarbio, C.F.Y.; Taboada, E.B. & Lacks, D.J. Extraction of bioactive compounds from mango (*Mangifera indica* L. var. Carabao) seed kernel with ethanol–water binary solvent systems. *J. Food Sci. Tech*., 2019, **56**, 2536-2544. doi: 10.1007/s13197-019-03732-7
17. Okwunodulu, F.U.; Chukwuemeka-Okorie, H.O. & Okorie, F.C. Biological synthesis of cobalt nanoparticles from mangifera indica leaf extract and application by detection of manganese (II) ions present in industrial wastewater. *Chem. Sci. Int. J*., 2019, **27**(1), 1-8.
18. Priyadarshini, S.; Bhol, R.; Sulava, S. & Jena, S. Green synthesis of silver nanoparticles by using mangifera indica and aegle marmelos leaf extract. *J. Cell Tissue Res*., 2020, **20**(1), 6889-6896.
19. Yahya, S.M.; Abdulmumin, Y.; Abdulmumin, T.M.; Sagagi, B.S.; Murtala, M.; Salau, A.K. & Hassan, S.A. Biological synthesis, characterisation and antimicrobial effect of silver nanoparticles (Ag-NPs) using aqueous extract of mango pulp (*Mangifera indica*). *J. Altern. Complement. Med*., 2021, **13**(4), 39-50. doi: 10.9734/JOCAMR/2021/v13i430233
20. Aniqa & Rizvi, Z.F. Physio-chemical analysis and antioxidative response of Ag NPs synthesised by sufaid chonsa mango pulp extracts of different ripening stages. *Sci. Rep*., 2024, **14**(1), 28514. doi: 10.1038/s41598-024-78725-4
21. Salati, S.; Doudi, M. & Madani, M. The biological synthesis of silver nanoparticles by mango plant extract and its anti-*candida* effects. *J. Appl. Biotechnol. Rep*, 2018, **5**(4), 157-161. doi: 10.29252/JABR.05.04.04
22. Elmosallamy, A.; El-zaidy, M. & Hussein, S. Green synthesis of silver nanoparticles using mangifera indica L. (Musk) peels extract and evaluation of its cytotoxic activities. *Egypt. J. Chem*., 2022, **65**(7), 447-455. doi: 10.21608/ejchem.2021.109739.5004
23. Jabin, T.; Biswas, S.; Islam, S.; Sarker, S.; Afroze, M.; Paul, G. K. & Zaman, S. (). Effects of gamma-radiation on microbial, nutritional, and functional properties of Katimon mango peels: A combined biochemical and in silico studies. *Heliyon*, 2023, **9**(11). doi: 10.1016/j.heliyon.2023.e21556
24. Núñez Sellés, A.J.; Vélez Castro, H.T.; Agüero-Agüero, J.; González-González, J.; Naddeo, F.; De Simone, F. & Rastrelli, L. Isolation and quantitative analysis of phenolic antioxidants, free sugars, and polyols from mango (*Mangifera indica* L.) stem bark aqueous decoction used in cuba as a nutritional supplement. *J. Agr. Food Chem*., 2002, **50**(4), 762-766. doi: 10.1021/jf011064b
25. Shaikh, J.R. & Patil, M. Qualitative tests for preliminary phytochemical screening: An overview. *Int. J. Chem. Stud*., 2020, **8**(2), 603-608. doi: 10.22271/chemi.2020.v8.i2i.8834
26. Archana, S.; Jayanna, B.K.; Ananda, A.; Shilpa, B.M.; Pandiarajan, D.; Muralidhara, H.B. & Kumar, K.Y. Synthesis of nickel oxide grafted graphene oxide nanocomposites-A systematic research on chemisorption of heavy metal ions and its antibacterial activity. *Environ. Nanotechnol. Monit. Manag*., 2021, **16**, 100486. doi: 10.1016/j.enmm.2021.100486
27. Yadav, L.R.; Shilpa, B.M.; Suma, B.P.; Venkatesh, R. & Nagaraju, G. Synergistic effect of photocatalytic,

antibacterial and electrochemical activities on biosynthesised zirconium oxide nanoparticles. *Eur. Phys. J. Plus*., 2021, **136**, 1-17. doi: 10.1140/epjp/s13360-021-01606-6.
28. Ananda, A.; Ramakrishnappa, T.; Archana, S.; Yadav, L.R.; Shilpa, B.M.; Nagaraju, G. & Jayanna, B.K. Green synthesis of MgO nanoparticles using *Phyllanthus emblica* for evans blue degradation and antibacterial activity. *Mater. Today: Proceedings*., 2022, **49**, 801-810. doi: 10.1016/J.MATPR.2021.05.340
29. Bharathi, V.; Firdous, J.; Muhamad, N.; & Mona, R. Green synthesis of *Mangifera indica* silver nanoparticles and its analysis using Fourier transform infrared and scanning electron microscopy. *National Natl. J. Physiol. Pharm. Pharmacol*., 2017, **7**(12), 1364-1367. doi: 10.5455/njppp.2017.7.0725428082017
30. Kora, A.J.; Mounika, J. & Jagadeeshwar, R. Rice leaf extract synthesised silver nanoparticles: An in vitro fungicidal evaluation against *Rhizoctonia solani*, the causative agent of sheath blight disease in rice. *Fungal Biol*., 2020, **124**(7), 671-681. doi: 10.1016/j.funbio.2020.03.012
31. Kumar, M.; Saurabh, V.; Tomar, M.; Hasan, M.; Changan, S.; Sasi, M.; Maheshwari, C.; Prajapati, U.; Singh, S.; Prajapat, R.K.; Dhumal, S.; Punia, S.; Amarowicz, R. & Mekhemar, M. Mango (*Mangifera indica* L.) Leaves: Nutritional composition, phytochemical profile, and health-promoting bioactivities. antioxidants (Basel, Switzerland). 2021, **10**(2), 299. doi: 10.3390/antiox10020299
32. Becheri, A.; Dürr, M.; Lo Nostro, P. *et al.* Synthesis and characterisation of zinc oxide nanoparticles: Application to textiles as UV-absorbers. *J. Nanopart. Res*., 2008, **10**, 679–689. doi: 10.1007/s11051-007-9318-3
33. Tripathy, A.; Raichur, A.M.; Chandrasekaran, N. *et al.* Process variables in biomimetic synthesis of silver nanoparticles by aqueous extract of *Azadirachta indica* (Neem) leaves. *J. Nanopart. Res*. 2010, **12**, 237–246. doi: 10.1007/s11051-009-9602-5
34. Donga, S. & Chanda, S. Facile green synthesis of silver nanoparticles using *Mangifera indica* seed aqueous extract and its antimicrobial, antioxidant and cytotoxic potential (3-in-1 system). *Artif. Cells Nanomed. Biotechnol*., 2021, **49**(1), 292–302. doi: 10.1080/21691401.2021.1899193
35. Niraimathi, K.L.; Sudha, V.; Lavanya, R. & Brindha, P. Biosynthesis of silver nanoparticles using *Alternanthera sessilis* (Linn.) extract and their antimicrobial, antioxidant activities. *Colloids Surf. B: Biointerfaces*., 2013, **102**, 288-291. doi: 10.1016/j.colsurfb.2012.08.041
36. Daisy, P. & Saipriya, K. Biochemical analysis of *Cassia fistula* aqueous extract and phytochemically synthesised gold nanoparticles as hypoglycemic treatment for diabetes mellitus. *Int. J. Nanomedicine*., 2012, 1189-1202. doi: 10.2147/IJN.S26650
37. Netala, V.R.; Kotakadi, V.S.; Domdi, L.; Gaddam, S.A.; Bobbu, P.; Venkata, S.K. & Tartte, V. Biogenic silver nanoparticles: Efficient and effective antifungal agents. *Appl. Nanosci*., 2016, **6**, 475-484. doi: 10.1007/s13204-015-0463-1.
38. Jaffri, S.B. & Ahmad, K.S. Augmented photocatalytic, antibacterial and antifungal activity of prunosynthetic silver nanoparticles. *Artif. Cells Nanomed. Biotechnol*., 2018, **46**(sup1), 127-137. doi: 10.1080/21691401.2017.1414826
39. Magudapathy, P.; Gangopadhyay, P.; Panigrahi, B.K.; Nair, K.G.M. & Dhara, S. Electrical transport studies of Ag nanoclusters embedded in glass matrix. *Phys. B: Condens. Matter*., 2001, **299**(1-2), 142-146. doi: 10.1016/S0921-4526(00)00580-9.
40. Muruganandam, S.; Anbalagan, G. & Murugadoss, G. Optical, electrochemical and thermal properties of Co^{2+}-doped CdS nanoparticles using polyvinylpyrrolidone. *Appl. Nanosci*., 2015, **5**, 245–253. doi: 10.1007/s13204-014-0313-6
41. Kokila, T.; Ramesh, P.S. & Geetha, D.J.A.N. Biosynthesis of silver nanoparticles from cavendish banana peel extract and its antibacterial and free radical scavenging assay: A novel biological approach. *Appl. Nanosci*., 2015, **5**, 911-920. doi: 10.1007/s13204-015-0401-2
42. Patil, M.P.; Rokade, A.A.; Ngabire, D. & Kim, G.D. Green synthesis of silver nanoparticles using water extract from galls of *Rhus chinensis* and its antibacterial activity. *J. Clust. Sci*., 2016, **27**, 1737-1750. doi: 10.1007/s10876-016-1037-4.
43. Marwal, A. & Gaur, R.K. Plant viruses as an engineered nano vehicle (PVENVs). *In*, Plant virus-host interaction, (Second Edition), *molecular approaches and viral evolution.,* 2021, **2**, 525-536. doi: 10.1016/B978-0-12-821629-3.00012-9
44. Tailor, S.; Jain, K.; Marwal, A.; Meena, M.; Anbarasu, K. & Gaur, R.K. Outlooks of nanotechnology in organic farming management. *Def. Life Sci. J.,* 2022, **7**(1), 52-60. doi: 10.14429/dlsj.7.16763
45. Meena, M.; Zehra, A.; Swapnil, P.; Harish.; Marwal, A.; Yadav, G. & Sonigra, P. Endophytic nanotechnology: An approach to study scope and potential applications. *Front. Chem*., 2021, **9**, 613343. doi: 10.3389/fchem.2021.613343

ACKNOWLEDGEMENT

The authors would like to thank Prof. R.P. Singh and his research scholar, Ms. Anshu Mathur (Microbial Biotechnology Laboratory), Department of Biosciences and Bioengineering, IIT, Roorkee for providing the facility for SEM, XRD, and EDX sample preparation and analysis.

CONTRIBUTORS

Ms. Shalini Tailor is pursuing her PhD in green synthesis of nanoparticles and structural based insilico drug designing from Department of Biotechnology, MLSU.

She has contributed in Material preparation, Data- curation and analysis, investigation, Writing-original draft, commented on previous versions of the manuscript. Ms. Shalini read and approved the final manuscript.

Ms. Ayushi Malik is pursuing her PhD in green synthesis of nanoparticles and structural based insilico drug designing from Department of Biotechnology, MLSU.
She has contributed in Data- curation and analysis, investigation, commented on previous versions of the manuscript. Ms. Ayushi read and approved the final manuscript.

Prof. (Dr.) R.K. Gaur earned his PhD in 2005 and currently working as Professor and Head at the Department of Biotechnology, Deen Dayal Upadhyaya Gorakhpur university, Gorakhpur, Uttar Pradesh, India.
His area of interest includes molecular characterisation of sugarcane viruses, viz., mosaic, streak mosaic and yellow luteovirus. He has contributed in XRD data interpretation, Writing – second draft, review & editing, commented on previous versions of the manuscript. Prof Gaur read and approved the final manuscript.

Dr. Avinash Marwal earned his PhD in 2014 and currently working as an Assistant Professor in the Department of Biotechnology, Mohanlal Sukhadia University, Udaipur, Rajasthan, India. He has expertise in molecular virology, host virus interactions, bioinformatics, and nano-biotechnology.
He has contributed in Supervision, Conceptualisation, Methodology, Resources, Writing – original draft, Writing – second draft, review & editing, Project administration, supervision, commented on previous versions of the manuscript. Dr. Marwal read and approved the final manuscript.